

# Wireless Strain and Crack Sensing Using a Folded Patch Antenna

Xiaohua Yi, Chunhee Cho, Chia-Hung Fang,  
Yang Wang, Roberto T. Leon  
School of Civil and Environment Engineering  
Georgia Institute of Technology  
Atlanta, GA, 30332

James Cooper, Rushi Vyas, Vasileios Lakafosis,  
Manos M. Tentzeris  
School of Electrical and Computer Engineering  
Georgia Institute of Technology  
Atlanta, GA, 30332

**Abstract**— In this research, folded patch antennas are investigated as low-cost and wireless smart-skin sensors that monitor the strain and crack in metallic structures. A radio frequency identification (RFID) chip is used for signal modulation. When the antenna is under strain/deformation, its resonance frequency varies accordingly. The variation can be easily interrogated and recorded by a reader that wirelessly delivers power for the antenna operation. Therefore, the antenna sensor can measure strain/crack. This paper reports latest test results on the strain and crack sensing performance of the antenna. In particular, tensile tests show that the wireless antenna sensor can detect small strain changes lower than  $20 \mu\epsilon$ , and can perform well at large strains higher than  $10,000 \mu\epsilon$ . In the crack test, a growing sub-millimeter crack is successfully detected by the antenna sensor.

**Keywords:** *Folded patch antenna; RFID; antenna sensor; wireless strain sensing; crack sensing*

## I. INTRODUCTION

Nearly one third of bridges in the U.S. are made of steel and aluminum iron, among which almost one quarter are rated as structurally deficient or functionally obsolete [1]. For all deficient bridges, fatigue-induced fracture/crack is among the most common concerns for inspectors and owners [2]. Current biennial bridge deck evaluation and assessment methods are mainly based on visual inspection [3], which cannot detect small-size cracks hidden under paint. The cracks may grow to critical and dangerous sizes before the next inspection cycle. Some existing technologies, including metal foil strain gages, fiber optic sensors, or ultrasonic testing, may assist in crack monitoring. However, most sensing systems either are too expensive for very dense instrumentation, or involve human-operated equipment that is not convenient for in-situ continuous deployment. These limitations make the existing technologies not practical for large-scale/large-area deployment and continuous monitoring in the field.

To address these difficulties, a radio frequency identification (RFID)-based folded patch antenna is developed as a passive wireless strain/crack sensor for metallic structures [4]. The system utilizes backscattering mechanism and adopts a low-cost RFID chip to reduce the design and manufacturing cost. Particularly, the RFID-based technology allows the antenna sensor to be passive, i.e. to operate without any other power source such as batteries [5].

In this research, an extensive suite of tests are devised and conducted to characterize the strain and crack sensing performance of the antenna sensor. The rest of the paper is organized as follows. First, the design and manufacturing of the antenna sensor are summarized. Then, experimental results are presented to illustrate the sensing performance in terms of strain resolution, strain measurement range, and crack detection.

## II. RFID TAG DESIGN

An RFID-based folded patch antenna is designed as the passive wireless strain/crack sensor [4]. Fig. 1 shows a 3D illustration of the antenna sensor design. Dimensions of the patch are marked in the figure. A patch antenna form is adopted to provide good radiation performance on metallic structures on which the sensor is to be installed. To further reduce the size of the antenna, vias through the substrate are used for connecting top copper cladding with ground plane on the back, forming a folded patch antenna. The substrate material is Rogers RT/duroid<sup>®</sup>5880 with a thickness of 0.79 mm. The RFID chip is an SL3ICS1002 model made by NXP Semiconductors. When impedance of the RFID chip equals complex conjugate of the antenna impedance, the RF circuit is matched and provides a resonance frequency. The resonance frequency of the antenna,  $f_{R0}$ , can be estimated as:

$$f_{R0} = \frac{c}{4(L + L')\sqrt{\epsilon_r}} \quad (1)$$

where  $c$  is the speed of light,  $L$  is the electrical length of the

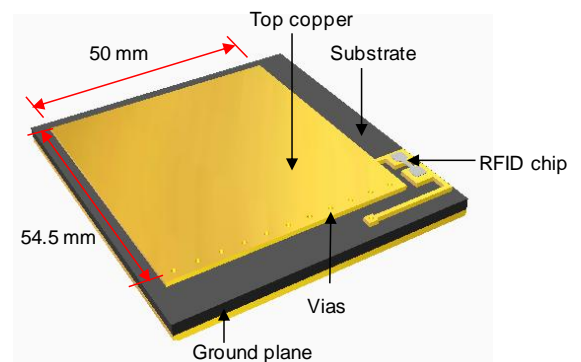


Fig. 1 RFID-based wireless antenna sensor

antenna,  $L'$  is additional length compensation due to fringing effect, and  $\epsilon_r$  is the substrate dielectric constant. When the antenna sensor experiences strain or crack that changes length  $L_0$ , antenna resonance frequency changes accordingly. Engineering strain is defined as relative change in length:

$$\epsilon = \frac{l - L_0}{L_0} \quad (2)$$

where  $L_0$  is original dimension of a material body;  $l$  is the final deformed dimension, along the same direction of  $L_0$ . The unit of strain is dimensionless, which is usually denoted as  $\mu\epsilon$  (microstrain).  $1 \mu\epsilon$  means  $1 \times 10^{-6}$  or 1 ppm (parts per million) relative change in length  $L_0$ .

The resonance frequency shift can be captured by an RFID reader. The Tagformance Lite reader unit, made by Voyantic Ltd., is adopted in this work. The reader is capable of measuring interrogation power threshold at each strain level, from which resonance frequency can be derived. The interrogation power threshold refers to the minimum required interrogation power from the reader, in order to activate RFID chip and receive response from the antenna sensor.

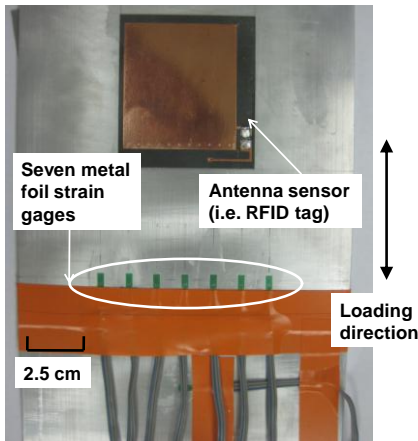


Fig. 2 Aluminum specimen configuration

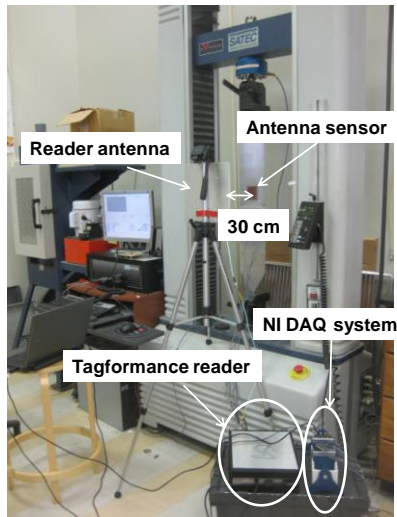


Fig. 3 Experimental setup

### III. EXPERIMENTAL RESULTS FOR STRAIN AND CRACK SENSING

Extensive tests for the antenna sensor are conducted to determine the strain sensing resolution, strain measurement range, and crack sensing capability.

#### A. Strain measurement resolution test

Fig. 2 shows an example aluminum specimen for strain measurement resolution and range tests, where one antenna sensor and seven metal foil strain gages (for baseline measurement) are installed in the center area of the specimen. Fig. 3 shows the complete experimental setup. Connected to a computer through a USB 2.0 cable, the Tagformance Lite reader antenna is placed 30 cm away from the antenna sensor. The metal foil strain gages are connected with a strain data acquisition system from National Instruments (NI 9135). In the experiment for measurement resolution, force applied by a tensile test machine is adjusted to generate about  $20 \mu\epsilon$  increment at each loading step. Interrogation power threshold plots measured at different strain levels are shown in Fig. 4. For clarity, only three strain levels are plotted. A fourth order curve fitting is applied to the valley area of these measurement curves to have more accurate determination for resonance frequency  $f_R$ . The resonance frequency change is then normalized by initial resonance frequency ( $f_{R0}$  at zero strain level) according to the following equation:

$$\Delta f_N = \frac{f_R - f_{R0}}{f_{R0}} \quad (3)$$

where  $\Delta f_N$  represents normalized frequency change. An approximately linear relationship is demonstrated between the normalized frequency change and the applied strain as shown in Fig. 5. The slope value of  $-0.7404 \text{ ppm}/\mu\epsilon$  is the normalized strain sensitivity. This means that  $1 \mu\epsilon$  strain causes the resonance frequency of the antenna sensor to reduce by  $0.7404 \text{ ppm}$ .

#### B. Strain measurement range test

Strain measurement range test is conducted using similar experimental setup as shown in Fig. 2 and Fig. 3. Fig. 6 shows the interrogation power threshold for strain measurement range experiment. For clarity, only five strain levels are shown in this figure. During this experiment, loading steps are configured to increase the strain up to  $10,000 \mu\epsilon$ . The normalized frequency change is shown in Fig. 7. The normalized strain sensitivity

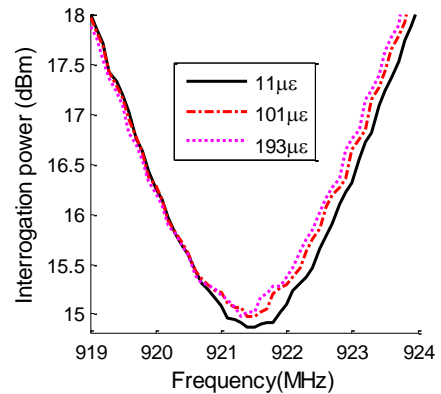


Fig. 4 Interrogation power threshold plot

remains consistent when the strain is less than 4,000  $\mu\epsilon$ , which is  $-0.7542 \text{ ppm}/\mu\epsilon$  for strain range between 0 and 1,000  $\mu\epsilon$  and  $-0.7784 \text{ ppm}/\mu\epsilon$  between 1,000  $\mu\epsilon$  and 4,000  $\mu\epsilon$ . The sensitivity value is also close to that shown in Fig. 5. When the applied strain is higher than 4,000  $\mu\epsilon$ , the normalized strain sensitivity is reduced to  $-0.382 \text{ ppm}/\mu\epsilon$ . The reduction is due to the yielding of aluminum specimen and the copper claddings on the antenna sensor. In addition, the dielectric property change of the Rogers 5880 substrate needs future investigation.

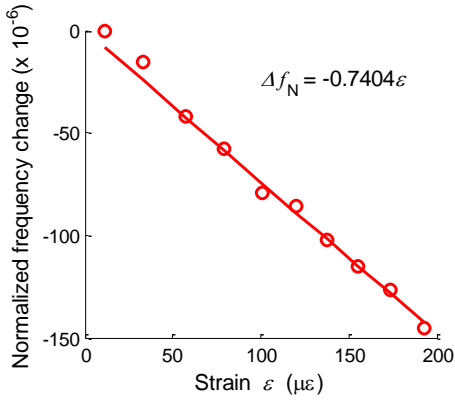


Fig. 5 Strain sensing resolution results

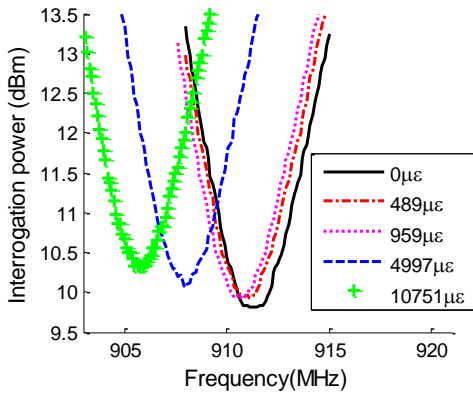


Fig. 6. Interrogation power threshold plots under different strain levels

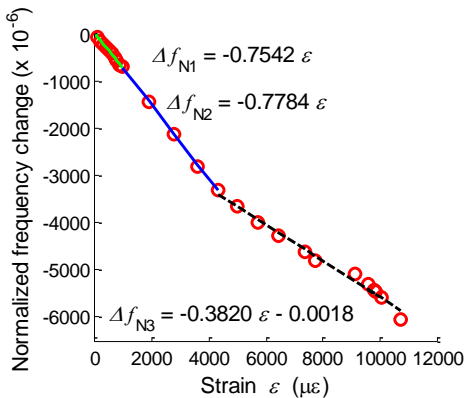


Fig. 7. Strain sensing measurement range results

### C. Crack measurement

Crack sensing experiment is conducted by a specially design crack testing device [6], which is shown in Fig. 8. Two aluminum plates, an upper rotating plate and a lower fixed plate, are installed on an aluminum base plate. The upper rotating plate can rotate along a rotating bolt at the bottom right, which is fastened to the base plate. Meanwhile, a fine-resolution displacement control screw (1.06 mm threading) is installed at the upper left of the rotating plate. By turning the screw, a rotation is imposed on the upper plate and a crack is opened between the upper and lower plates. The crack opening size is measured by a digital dial gage (0.00254 mm resolution)

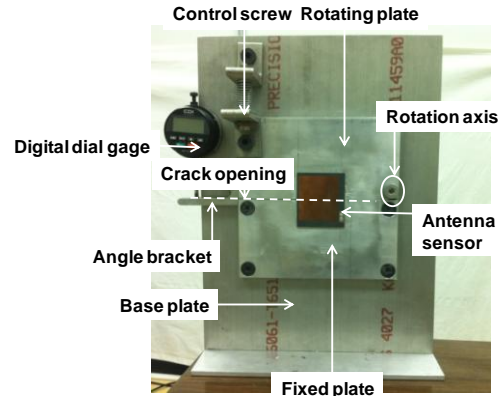


Fig. 8 Crack testing device

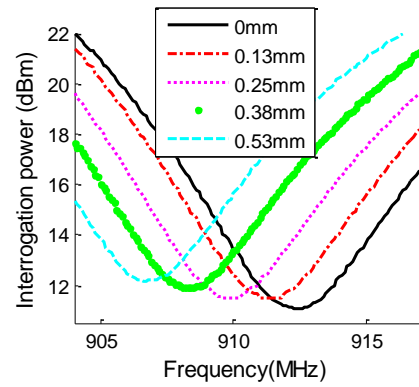


Fig. 9. Interrogation power threshold plots under different crack opening sizes

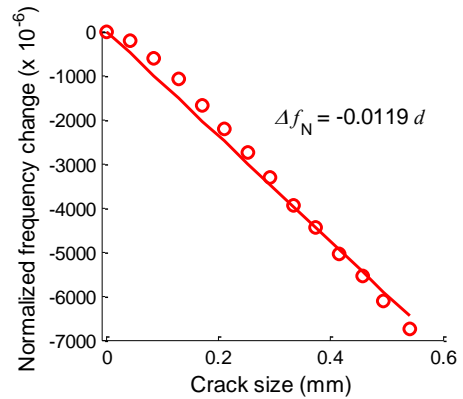


Fig. 10 Crack sensing results

mounted at the left side of the base plate. A spring-loaded probe from the gage pushes against an angle bracket that is fastened to the left edge of the rotating plate.

Fig. 9 shows interrogation power threshold plots under different crack sizes. As shown in this figure, resonance frequency of the antenna sensor decreases as the crack opening size increases. Fig. 10 shows the normalized frequency change as a crack opening widens under the antenna sensor. The normalized crack sensitivity is  $-0.0119$  ppm/mm, which means 1 mm crack underneath the sensor causes the resonance frequency to reduce by 0.0119 ppm. Fig. 11 shows



(a) 0.13 mm



(b) 0.53 mm



(c) 0.81 mm

Fig. 11. Photos of deformed antenna sensor at different crack opening sizes

representative photos of the antenna sensor at different crack opening sizes. Fig. 11(a) shows when the crack opening size is 0.13 mm. There is no actual crack observed in this scenario. Fig. 11(b) shows when the crack opening size is 0.53 mm. Small cracks can be observed in this scenario, which is the last step shown in Fig. 9. Fig. 11(c) shows when the opening is 0.81 mm, where a through crack is developed and no signal can be detected.

#### IV. CONCLUSIONS

This paper describes the strain measurement resolution, range, and crack sensing performance of a wireless battery-free antenna sensor. Sensor design and manufacturing are first described. To characterize strain and crack sensing performance, tensile and crack tests are conducted and measurement results are presented. Test results show that the antenna sensor can measure strain as small as  $20 \mu\epsilon$  and as high as  $10,000 \mu\epsilon$ . In addition, the antenna sensor is capable of measuring sub-millimeter crack and tracking its propagation.

Since the wireless interrogation distance is related with antenna gain of the reader antenna, the interrogation distance can be increased with higher gain for the reader antenna. More experiments will be conducted to explore the sensing performance using different reader antennas. Meanwhile, different crack propagation scenarios can be studied and tested.

#### ACKNOWLEDGMENT

This material is based upon work supported by the Federal Highway Administration under agreement No. DTFH61-10-H-00004. Any opinions, findings, and conclusions or recommendations expressed in this publication are those of the authors and do not necessarily reflect the view of the Federal Highway Administration.

#### REFERENCES

- [1] FHWA, National Bridge Inventory. U.S. Department of Transportation, Federal Highway Administration, Washington D.C. 2011.
- [2] ASCE, Report Card for America's Infrastructure. Reston, VA: American Society of Civil Engineers, 2009.
- [3] AASHTO, Manual of Bridge Evaluation. American Association of State Highway & Transportation Officials, Washington D.C. 2009.
- [4] X. Yi, T. Wu, Y. Wang, R. T. Leon, M. M. Tentzeris, and G. Lantz, "Passive wireless smart-skin sensor using RFID-based folded patch antennas," *International Journal of Smart and Nano Materials*, vol. 2, pp. 22-38, 2011.
- [5] K. Finkenzeller, *RFID Handbook*. 2nd ed. New York: John Wiley & Sons, 2003.
- [6] X. Yi, J. Cooper, Y. Wang, M. M. Tentzeris, and R. T. Leon, "Wireless crack sensing using an RFID-based folded patch antenna," in *Proceeding of the 6th International Conference on Bridge Maintenance, Safety and Management (IABMAS 2012)*, Lake Como, Italy, 2012.